

Chemical Reactions on Surface Molecules Attached to Silicon Quantum Dots

Amane Shiohara,[†] Sanshiro Hanada,[‡] Sujay Prabakar,[†] Kohki Fujioka,[†]
Teck H. Lim,[†] Kenji Yamamoto,[‡] Peter T. Northcote,[†] and Richard D. Tilley^{*,†}

School of Chemical and Physical Sciences, MacDiarmid Institute of Advanced Materials and Nanotechnology, Victoria University of Wellington, P.O. Box 600, Wellington, New Zealand, and International Clinical Research Centre, Research Institute, International Medical Centre of Japan, 1-21-1 Toyama, Shinjuku-ku, Tokyo, 162-8655 Japan

Received August 1, 2009; E-mail: richard.tilley@vuw.ac.nz

Abstract: This Article describes research on chemical reactions on molecules attached to the surface of silicon quantum dots that have been performed to produce quantum dots with reactive surface functionalities such as diols and epoxides. Characterization of the surface reactions includes NMR and FT-IR studies, and the quantum dots were characterized by transmission electron microscopy (TEM) and energy dispersive spectroscopy (EDS). Cytotoxicity and cell viability assay conducted on silicon dots capped with polar molecules indicated low toxicity with quantum dots with more reactive functionalities found to be more toxic. The silicon quantum dots photoluminesce and have been used as a blue chromophore for the biological imaging of cells.

Introduction

Quantum dots have several interesting characteristics due to quantum effects that appear at the nanoscale. They have unique optical and electronic properties that are not observed in their bulk counterparts.¹ Because of these characteristics, they have found many applications including in lasers, photosensors, and medical biology.^{2–16} Current medical and biological fluorescent imaging is limited to the use of conventional organic dye

markers, which have limited photostability. Recently, these have begun to be replaced by quantum dots of materials such as cadmium selenide (CdSe), silicon, and germanium that have several advantages including enhanced photostability.^{17–21}

Quantum dots of group II/VI such as CdSe quantum dots are well-known, and substantial research has been conducted on these systems because of their strong luminescence.²¹ There have, however, been concerns over the toxicity of these quantum dots in the human body. The toxicity of these quantum dots arises from two main sources: (1) the quantum dot core and (2) the capping molecules.

The cytotoxicity of CdSe quantum dots has been reported by Derfus et al.²² who illustrated that cell damage could be caused by an uncoated CdSe core under UV excitation. Because of their low toxicity, silicon nanoparticles would be an ideal candidate for biological fluorescence imaging. Silicon has the advantage of being nontoxic and inexpensive, and, over the past few decades, many methods for the synthesis of silicon and germanium quantum dots have been reported. The solution-phase synthesis of silicon quantum dots via a reductive process has been reported by Kauzlarich and co-workers,^{23–34} at high

[†] Victoria University of Wellington.

[‡] International Medical Centre of Japan.

- (1) Alivisatos, P. A. *J. Phys. Chem.* **1996**, *100*, 13226–13239.
- (2) Alivisatos, P. A. *Science* **1996**, *271*, 933.
- (3) Bruchez, M., Jr.; Moronne, M.; Gin, P.; Weiss, S.; Alivisatos, P. A. *Science* **1998**, *281*, 2013–2016.
- (4) Chan, W. C. W.; Nie, S. *Science* **1998**, *281*, 2016–2018.
- (5) Mattousi, H.; Mauro, J. M.; Goldman, E. R.; Anderson, G. P.; Sundar, C. V.; Mikulec, V. F.; Bawendi, G. M. *J. Am. Chem. Soc.* **2000**, *122*, 12142–12150.
- (6) Dubertret, B.; Skourides, P.; Norris, D. J.; Noireaux, V.; Brivanlou, A. H.; Libchaber, A. *Science* **2002**, *298*, 1759–1762.
- (7) Alivisatos, P. A. *Nat. Biotechnol.* **2004**, *22*, 47–52.
- (8) Hoshino, A.; Hanaki, K.; Suzuki, K.; Yamamoto, K. *Biochem. Biophys. Res. Commun.* **2004**, *314*, 46–53.
- (9) Hanaki, K.; Momo, A.; Oku, T.; Komoto, A.; Maenosono, S.; Yamaguchi, Y.; Yamamoto, K. *Biochem. Biophys. Res. Commun.* **2003**, *302*, 496–501.
- (10) Al-Salim, N.; Young, A. G.; Tilley, R. D.; McQuillan, A. J.; Xia, J. *Chem. Mater.* **2007**, *19*, 5185–5193.
- (11) Coe, S.; Woo, W. K.; Bawendi, M. G.; Bulovic, V. *Nature* **2002**, *420*, 800–803.
- (12) Santori, C.; Fattal, D.; Vickovic, J.; Solomon, G. S.; Yamamoto, Y. *Nature* **2002**, *419*, 594–597.
- (13) Harman, T. C.; Taylor, P. J.; Walsh, M. P.; LaForge, B. E. *Science* **2002**, *297*, 2229–2232.
- (14) Li, X.; Wu, Y.; Steel, D.; Gammon, D.; Stievater, T. H.; Katzer, D. S.; Park, D.; Piermarocchi, C.; Sham, L. J. *Science* **2003**, *301*, 809–811.
- (15) Beham, E.; Stuffer, S.; Findeis, F.; Bichler, M.; Abstreiter, G.; Zrenner, A. *Nature* **2002**, *418*, 612–614.
- (16) Xu, S.; Kumar, S.; Nann, T. *J. Am. Chem. Soc.* **2006**, *128*, 1054–1055.

- (17) Che, J.; Wang, X.; Xiao, Y.; Wu, X.; Zhou, L.; Yuan, W. *Nanotechnology* **2007**, *18*, 135706.
- (18) Alsharif, N. H.; Berger, C. E. M.; Varanasi, S. S.; Chao, Y.; Horrocks, B. R.; Datta, H. K. *Small* **2009**, *5*, 221–228.
- (19) Zou, J.; Kauzlarich, S. M. *J. Cluster Sci.* **2008**, *19*, 341–355.
- (20) Warner, J. H.; Tilley, R. D. *Nanotechnology* **2006**, *17*, 3745–3749.
- (21) Nirmal, M.; Dabbousi, B. O.; Bawendi, M. G.; Macklin, J. J.; Trautman, J. K.; Harris, T. D.; Brus, L. E. *Nanotechnology* **1996**, *383*, 802–804.
- (22) Derfus, A. M.; Chan, W. C. W.; Bhatia, S. N. *Nano Lett.* **2004**, *4*, 11–18.
- (23) Neiner, D.; Chiu, H. W.; Kauzlarich, S. M. *J. Am. Chem. Soc.* **2006**, *128*, 11016–11017.
- (24) Baldwin, R. K.; Zou, J.; Pettigrew, K. A.; Yeagle, G. J.; Britt, R. D.; Kauzlarich, S. M. *Chem. Commun.* **2006**, *6*, 658–660.

temperatures and pressures by Korgel and co-workers,^{35–40} and microemulsion synthesis.^{41,42}

The surface modification of silicon quantum dots is very important to impart functionalities. Because silicon quantum dots are able to be covalently bound to carbon- or oxygen-containing molecules, there are a few reports on silicon quantum dots capped with hydrophobic molecules such as 1-heptene.⁴³ The preparation of water-dispersible silicon quantum dots that maintain their photoluminescence stability has been proved to be difficult. Acrylic acid (PAAc) coated silicon quantum dots have been reported by Ruckenstein et al.⁴⁴ These silicon quantum dots were stable in aqueous solutions with good photoluminescent stability. Swihart et al.⁴⁵ also reported propionic acid coated silicon quantum dots. In both cases, silicon quantum dots were capped under UV light irradiation. We have reported the synthesis of amino-terminated silicon quantum dots made in reverse micelle system and capped with allylamine using a platinum catalyst.⁴⁶ However, reports describing the surface modification of silicon quantum dots are still few. Additionally, most of the surface capping protocols are single step processes in which the target molecules are directly attached onto the surface. In this study, our technique of surface modification is multistep based on the chemistry of the terminal double bond on the surface to achieve the target functionalities. The reason for adopting a stepwise approach is that when attaching functional molecules to the surface of silicon quantum dots some of the molecules tend to have more than one reactive moiety. For example, molecules with an oxygen containing functional group such as carboxylic group or hydroxy group and a double bond may preferentially react with the

oxygen functionality, not the carbon double bond. The approach we have adopted enables the formation of silicon quantum dots functionalized with a broad range of functional groups including highly reactive species such as epoxides.

Different surface modifications can induce different levels of quantum dot toxicity. Thus, a detailed examination of the toxicity of quantum dots with various capping molecules is essential for the widespread understanding of the application of quantum dots in biological imaging.

In this study, silicon quantum dots were synthesized by microemulsion synthesis. Silicon quantum dots were characterized by transmission electron microscopy (TEM) and energy dispersive spectrometry (EDS). Quantum dots were purified by liquid-phase separation and column chromatography. We also introduce methods for producing silicon quantum dots with different surface modifications with a view toward biomedical applications. The capping of the silicon quantum dots has been fully characterized using nuclear magnetic resonance (NMR) and Fourier transform infrared spectroscopy (FTIR). The cytotoxicity of quantum dots with different surface modifications has been evaluated, and the optimal surface capping in terms of lowest toxicity has been established.

Experimental Section

Synthesis of Surface Passivated Silicon Quantum Dots. All reactions were performed in a nitrogen filled glovebox. In a typical experiment, 0.002 mol of SiBr₄ (0.3 mL) was dissolved using a homogenizer in either 1.5 g of TOAB and 100 mL of anhydrous toluene or 1.5 g of C₁₂E₅ and 100 mL of anhydrous hexane. Hydrogen-terminated silicon nanoparticles were formed by adding a stoichiometric amount of reducing agent. Hydrophobic and hydrophilic particles were formed by modifying the surface silicon–hydrogen bonds by reaction with 92 μ L of 0.1 mol H₂PtCl₆ in isopropanol as catalyst and 4 mL of either allylamine or 1,5-hexadiene.

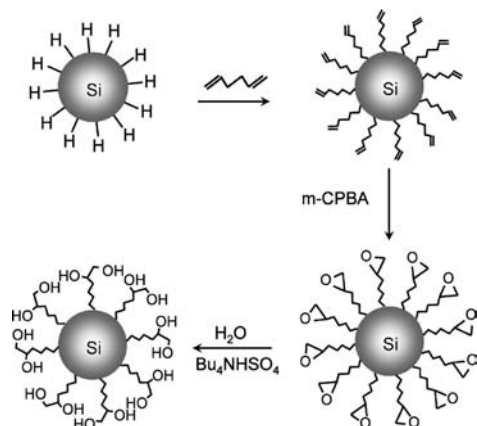
Purification of Silicon Quantum Dots. Liquid-phase separation was applied to alkene-terminated silicon quantum dots. All of the solvent was removed under vacuum, and 100 mL of hexane was added followed by 5 min sonication. The solution was transferred to a separation funnel and washed with *N*-methylformamide (Aldrich) three times. The organic layer was extracted and washed with water three times. The organic layer was then concentrated to give alkene-terminated silicon quantum dots.

Amine-terminated silicon quantum dots were purified by size exclusion column chromatography. The solvent was removed under vacuum, and 50 mL of methanol was added to dissolve the particles. The solution was sonicated for 5 min and filtered through a Millipore 0.45 μ m filter paper. The filtrate was concentrated down to 1 mL and was put into the column ($\phi = 1$ cm, 41.0 cm). Sephadex gel LH-20 (beads size 25–100 μ m) was used as the stationary phase. Flow rate was a drop per 5 s, and fractions were collected every 50 drops. Each fraction was checked for luminescence under a UV lamp (365 nm). The luminescent fraction was collected and concentrated down to 1 mL to give pure amine-terminated silicon quantum dots.

Chemical Reactions on the Surface of Silicon Quantum Dots. a. Epoxide-Terminated Silicon Quantum Dots. Epoxide-terminated silicon quantum dots were synthesized from alkene-terminated silicon quantum dots. 0.4 g (1.5 equiv) of chloroperoxy benzoic acid (*m*-CPBA; Aldrich) was added to a solution of alkene-terminated silicon quantum dots in 20 mL of CH₂Cl₂. The reaction mixture was stirred for 6 h and quenched with a saturated solution of Na₂SO₃. The aqueous phase was extracted with CH₂Cl₂, and the combined organic solution was washed with 10% NaOH solution. The organic layer was collected, and MgSO₄ was added to absorb water. The solution was filtered and concentrated under reduced pressure to give epoxide-terminated silicon quantum dots.

- (25) Zou, J.; Baldwin, R. K.; Pettigrew, K. A.; Kauzlarich, S. M. *Nano Lett.* **2004**, *4*, 1181–1186.
- (26) Tanke, R. S.; Kauzlarich, S. M.; Patten, T. E.; Pettigrew, K. A.; Murphy, D. L.; Thompson, M. E.; Lee, H. W. H. *Chem. Mater.* **2003**, *15*, 1682–1689.
- (27) Liu, Q.; Kauzlarich, S. M. *Mater. Sci. Eng., B* **2002**, *96*, 72–75.
- (28) Baldwin, R. K.; Pettigrew, K. A.; Ratai, E.; Augustine, M. P.; Kauzlarich, S. M. *Chem. Commun.* **2002**, *17*, 1822–1823.
- (29) Baldwin, R. K.; Pettigrew, K. A.; Garno, J. C.; Power, P. P.; Liu, G. Y.; Kauzlarich, S. M. *J. Am. Chem. Soc.* **2002**, *124*, 1150–1151.
- (30) Mayeri, D.; Phillips, B. L.; Augustine, M. P.; Kauzlarich, S. M. *Chem. Mater.* **2001**, *13*, 765–770.
- (31) Yang, C. S.; Bley, R. A.; Kauzlarich, S. M.; Lee, H. W. H.; Delgado, G. R. *J. Am. Chem. Soc.* **1999**, *121*, 5191–5195.
- (32) Zhang, X.; Brynda, M.; Britt, R. D.; Carroll, E. C.; Larsen, D. S.; Louie, A. Y.; Kauzlarich, S. M. *J. Am. Chem. Soc.* **2007**, *129*, 10668–10669.
- (33) Zhang, X.; Neiner, D.; Wang, S.; Louie, A. Y.; Kauzlarich, S. M. *Nanotechnology* **2007**, *18*, 9–095601.
- (34) Zou, J.; Sanelle, P.; Pettigrew, K. A.; Kauzlarich, S. M. *J. Cluster Sci.* **2006**, *17*, 565–578.
- (35) Lu, X. M.; Korgel, B. A.; Johnston, K. P. *Nanotechnology* **2005**, *16*, S389.
- (36) Lee, D. C.; Hanrath, T.; Korgel, B. A. *Angew. Chem., Int. Ed.* **2005**, *44*, 3573–3577.
- (37) Pell, L. E.; Schrickler, A. D.; Mikulec, F. V.; Korgel, B. A. *Langmuir* **2004**, *20*, 6546–6548.
- (38) Hanrath, T.; Korgel, B. A. *Adv. Mater.* **2003**, *15*, 437–440.
- (39) English, D. S.; Pell, L. E.; Yu, Z. H.; Barbara, P. F.; Korgel, B. A. *Nano Lett.* **2002**, *2*, 681–685.
- (40) Holmes, J. D.; Ziegler, K. J.; Doty, R. C.; Pell, L. E.; Johnston, K. P.; Korgel, B. A. *J. Am. Chem. Soc.* **2001**, *123*, 3743–3748.
- (41) Tilley, R. D.; Yamamoto, K. *Adv. Mater.* **2006**, *18*, 2053–2056.
- (42) Wilcoxon, J. P.; Samara, G. A.; Provencio, P. N. *Phys. Rev. B* **1999**, *60*, 2704–2714.
- (43) Tilley, R. D.; Warner, J. H.; Yamamoto, K.; Matsui, I.; Fujimori, H. *Chem. Commun.* **2005**, *14*, 1833–1835.
- (44) Li, Z. F.; Ruckenstein, E. *Nano Lett.* **2004**, *4*, 1463–1467.
- (45) Sato, S.; Swihart, M. T. *Chem. Mater.* **2006**, *18*, 4083–4088.
- (46) Warner, J. H.; Hoshino, A.; Yamamoto, K.; Tilley, R. D. *Angew. Chem., Int. Ed.* **2005**, *44*, 4550–4554.

Scheme 1. Reactions on Surface Molecules Bound to Silicon Quantum Dots



b. Diol-Terminated Silicon Quantum Dots. 8.5 mg (0.025 mmol) of phase transfer catalyst, tetrabutylammonium hydrogen sulfate (Bu_4NHSO_4), in H_2O (2.0 mL) was added to a solution of epoxide-terminated silicon quantum dots in CHCl_3 . The mixture solution was stirred for 24 h at 45 °C. The mixture was extracted with diethyl ether (3×10 mL), and the combined organic layer was dried over Na_2SO_4 . The solution was concentrated under reduced pressure to give diol-terminated silicon dots.

FTIR Spectroscopy. A Perkin-Elmer FT-IR spectrometer was used to identify and characterize the structure of the molecules attached to the nanoparticle surfaces. A KBr pellet was prepared by grinding powder KBr and a drop of each silicon quantum dot solution.

^1H NMR Spectroscopy. ^1H NMR (500 MHz) spectra of samples in CDCl_3 were recorded on a Varian Unity Inova 500 MHz spectrometer. The solvent of each sample solution was removed by evaporation using a rotary evaporator at 60 °C. After removal of the solvent, the sample was freeze-dried overnight and dissolved in CDCl_3 .

Cytotoxicity Evaluation. For the cytotoxicity assays, WS1, A549, and HepG2 cells were used. WS1 and A549 were tested for epoxide- and diol-terminated silicon quantum dots, and HepG2 was used for amine-terminated silicon quantum dots.

We inoculated 10 000 cells in each well of 96-well plates and cultured them for 48 h at 37 °C/5% CO_2 . Next, each type of silicon quantum dots was added in the indicated concentrations and cocultured for 48 h for WS1 and A549 cells and 1 h for HepG2 cells. The cytotoxicities of these quantum dots were examined in a cell viability assay. We used a Cell Counting Kit-8 (Dojindo, Japan) to measure the succinate dehydrogenase mitochondrial activity. The 450 nm absorption of formazans produced by the enzyme was measured with a DTX 880 (Beckman Coulter, Inc., USA) microplate reader ($n = 3$). The activities were calculated as the ratio of the absorbance value against those of the control.

Cell Imaging. Silicon quantum dots capped with allylamine were applied for cell imaging. HepG2 cells were used. The assay was conducted at 1.0 $\mu\text{g}/\text{mL}$ for 6 h incubation. The image was taken on a fluorescent microscope IX-81 (Olympus) with an excitation filter 330–380 nm.

Results and Discussion

Silicon quantum dots were synthesized by a microemulsion route. Silicon tetrabromide was used as the silicon precursor and reduced by strong hydride reducing agents. Hydrogen-terminated silicon quantum dots produced were capped with organic molecules by using a Pt-based catalyst or exposure to UV radiation.

The surface modification reactions performed are shown in Scheme 1. Alkene-terminated silicon quantum dots were

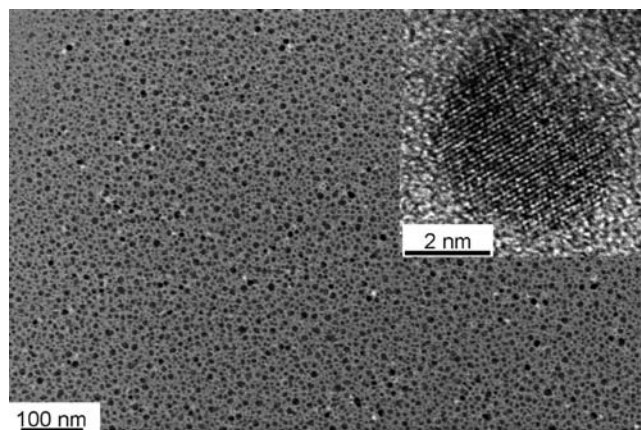


Figure 1. TEM image of amine-terminated silicon quantum dots and inset showing a high-resolution TEM image of an individual silicon nanocrystal.

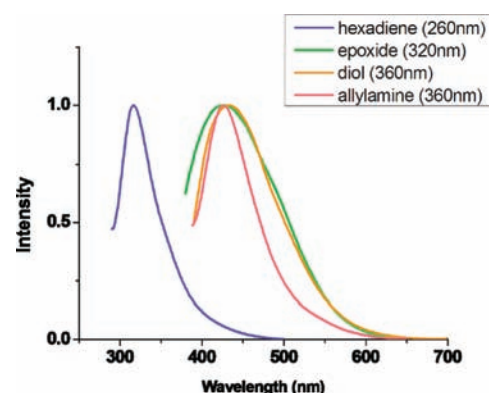


Figure 2. Photoluminescence spectra of silicon quantum dots capped with hexadiene-, epoxide-, diol-, and amine-terminated silicon quantum dots. Y axis shows normalized intensity.

synthesized by capping with 1,5-hexadiene. The direct reaction of hydride-terminated silicon quantum dots with alkenes containing alcohol and epoxide functional groups leads to complex reactions between the quantum dots and the oxygen functional group. Thus, epoxy-terminated and diol-terminated silicon quantum dots were synthesized by direct reaction of diene functional groups on the surface of the silicon quantum dots. Silicon quantum dots were reacted with allylamine to produce silicon quantum dots with amine functional groups on their surface.

Electron Microscopy. Figure 1 shows the TEM images of silicon quantum dots capped with allylamine. The amine capped silicon quantum dots produced ranged in size from 1.5 to 10 nm. The amine capped nanoparticles have an average diameter of 3.7 ± 0.9 nm, which is close to the exciton Bohr radius of silicon (4.3 nm). TEM images of the diene and diol samples are shown in Figures S-1 and S-2 (see the Supporting Information) and were similar in size to the amine capped silicon quantum dots having average sizes of 3.6 and 3.4 nm, respectively. From the TEM images, the particle sizes were relatively monodisperse, and aggregation of the nanoparticles was not observed. EDS analysis of the sample further confirmed the presence of silicon.

Optical Properties. Figure 2 shows the photoluminescence (PL) spectra of silicon quantum dots terminated with hexadiene, epoxy, diol, and amine functional groups. The nanoparticles were excited at 260 nm (hexadiene capped), 320 nm (epoxide-

terminated), and 360 nm (diol- and amine-terminated). The emission peak position of the silicon quantum dots capped with nonpolar hexadiene is around 320 nm. In comparison, the emission peak of silicon quantum dots capped with the polar functionalities, epoxide, diol, and allylamine, is around 430 nm. Full photoluminescence (PL) spectra of silicon quantum dots capped with hexadiene-, epoxy-, diol-, and amine-terminated silicon quantum dots over a range of excitation wavelengths are shown in Figure S-3 (see the Supporting Information). The absorption spectra of the silicon quantum dots with different surface terminations are shown in Figure S-4 (see the Supporting Information).

The origin of the photoluminescence in silicon quantum dots is complicated by the presence of both indirect and direct band gap transitions. The blue luminescence shown in Figure 2 has been previously observed for silicon quantum dots and can be attributed to the $\Gamma-\Gamma$ direct band gap transition and is in good agreement with previous reports.^{40,42,46,47}

The observation that silicon quantum dots capped with nonpolar diene have a higher energy emission than the quantum dots terminated with polar epoxy, diol, and amine functional groups is of interest and similar to previous observations comparing the optical properties of silicon quantum dots capped with nonpolar and polar molecules.⁴⁷ From the TEM images of these samples, shown in Figures 1, S-1, and S-2 (see the Supporting Information), it can be seen that the nanocrystal sizes are almost identical, and therefore the origin of the difference in the energy of the emission is most likely due to the nature of the surface capping and environment.⁴⁷ This result provides direct evidence that the surface-capping molecule plays an important role in the radiative recombination mechanisms in 2–4 nm silicon nanocrystals. The difference in the emission is most likely due to different radiative recombination pathways for polar and nonpolar capped silicon nanocrystals.⁴⁷ Theoretical studies have shown that it is possible for the electronic charge distribution of polar-capped silicon nanocrystals to be modified by the polar nature of cappings ligand, leading to the band gap being slightly lower for polar capped silicon nanocrystals than for nonpolar capped silicon nanocrystals, and this may be occurring in our samples.^{48–50}

FTIR Studies. To confirm the surface modification is successful, the nanoparticles were further characterized by FTIR and NMR. Figure 3 shows the FTIR spectra of alkene-, epoxy-, and diol-terminated silicon quantum dots, respectively.

For the hexadiene capped silicon quantum dots spectrum, Figure 3d, two peaks observed at 1460 and 1260 cm^{-1} are attributed to the vibrational scissoring and symmetric bending of $\text{Si}-\text{CH}_2$, respectively, and these peaks can be seen in all three spectra. This clearly indicates that one of the double bonds of hexadiene has reacted with the silicon–hydrogen bond on the surface of the quantum dots to form a silicon carbon bond. The peak at 1640 cm^{-1} of alkene-terminated silicon dot corresponds to the $\text{CH}_2=\text{CH}$ stretch vibration of the terminated double bond. This peak cannot be seen in the other two spectra.

In the spectrum of epoxy-terminated silicon quantum dots, Figure 3c, the peak of epoxy ring symmetrical stretching can be observed at 1217 cm^{-1} . The peak at 1640 cm^{-1} corresponding

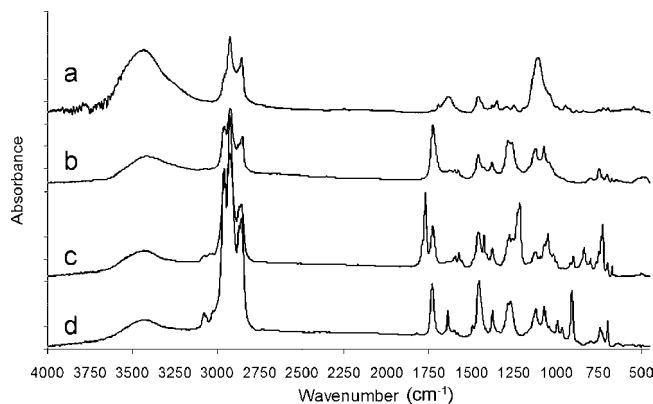


Figure 3. FTIR spectra of silicon quantum dots capped with (a) amine, (b) diol, (c) epoxy, and (d) diene.

to the $\text{CH}_2=\text{CH}$ terminated double bond has also disappeared, implying oxidation of the terminal double bond to the epoxide.

In Figure 3b, evidence for the hydrolytic ring-opening from the epoxy group to a diol is shown by the peak corresponding to an O–H vibration of an alcohol group as can be seen at 1285 cm^{-1} and the disappearance of the epoxide ring stretch.

For allylamine capped silicon quantum dots, Figure 3a, peaks observed at 1460 and 1248 cm^{-1} are attributed to $\text{Si}-\text{CH}_2$ vibrational scissoring and symmetric bending. The absorbance from 3500 to 3655 cm^{-1} is attributed to the N–H stretch of an amine. The peak at 1630 cm^{-1} is attributed to allylamine N–H scissoring. The peaks around 2850 and 2925 cm^{-1} represent alkane C–H stretching.

NMR Studies. The surface state of silicon quantum dots was also confirmed by NMR. Figure 4 shows the NMR spectra of each type of silicon quantum dot.

The peaks in Figure 4d, corresponding to the alkene-terminated quantum dots, at δ 4.85 (doublet, 9.0 Hz), δ 4.92 (doublet, 16.9 Hz), and δ 5.72 (multiplet) are typical of a terminal alkene and indicate the formation of silicon quantum dots with a free terminated alkene bond.

The peaks of the terminal alkene are absent in the spectrum of epoxy-terminated silicon quantum dots, Figure 4c, and are replaced by peaks at 2.39, 2.67, and 2.82 ppm, which indicate the presence of an epoxy ring and are similar to the peaks seen in free 1-epoxyhexane.

Upon hydrolysis of the epoxide to the diol, these peaks shift to slightly higher ppm, to 3.36–3.67 ppm consistent with the epoxide ring being opened, shown in Figure 4b.

The allylamine coated silicon quantum dots, Figure 4a, have a quartet peak between 3.70 to 3.75 ppm. This peak is attributed to the protons next to amine group. Also, the protons of the amine group were observed in the peak at 1.25 ppm. All of the NMR data were taken after removal of all volatile starting materials under vacuum at 60 °C. The boiling points of 1,5-hexadiene and allylamine are 60 and 53 °C, respectively; therefore, the peaks observed in the spectra were not from free capping molecules, which all have low boiling points, but from the surface moieties on the silicon quantum dots.

Cytotoxicity Evaluation. Cell viability assay (MTT assay) was applied for cytotoxicity evaluation. Human skin fibroblasts (WS1) and lung epithelial cells (A549) were used for epoxide-terminated and diol-terminated silicon quantum dot because the skin and lungs have higher possibilities of exposure through different mechanisms. The results of the cell viability assay are shown in Figure 5. As can be seen in the figure, epoxide-

(47) Warner, J. H.; Rubinsztein-Dunlop, H.; Tilley, R. D. *J. Phys. Chem. B* **2005**, *109*, 19064–19067.

(48) Reboredo, F. A.; Galli, G. *J. Phys. Chem. B* **2005**, *109*, 1072.

(49) Walker, B. G.; Hendy, S. C.; Gebauer, R.; Tilley, R. D. *Eur. Phys. J. B* **2008**, *66*, 7–15.

(50) Zhou, Z.; Brus, L.; Friesner, R. *Nano Lett.* **2003**, *3*, 163.

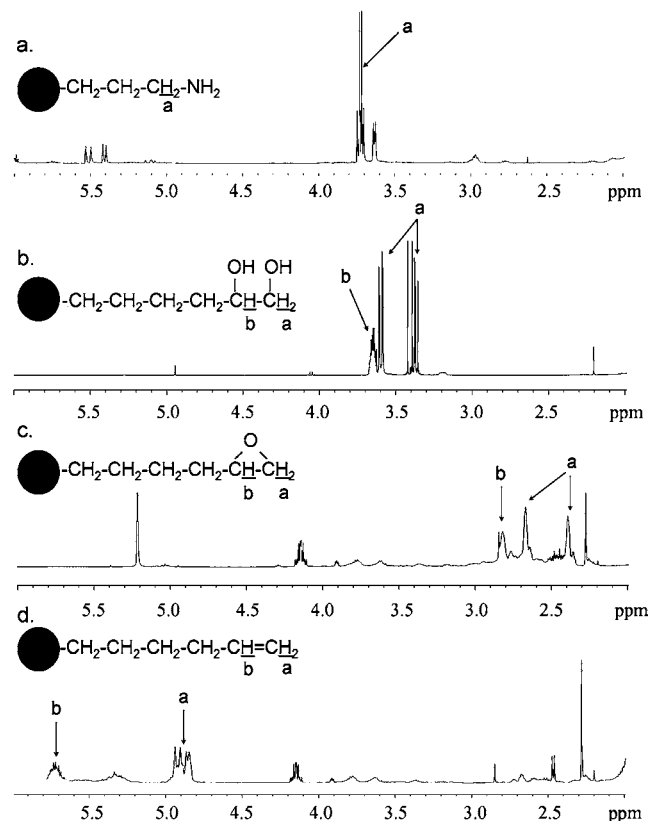


Figure 4. ^1H NMR spectra of silicon quantum dots capped with (a) amine, (b) diol, (c) epoxy, and (d) diene (500 MHz, CDCl_3).

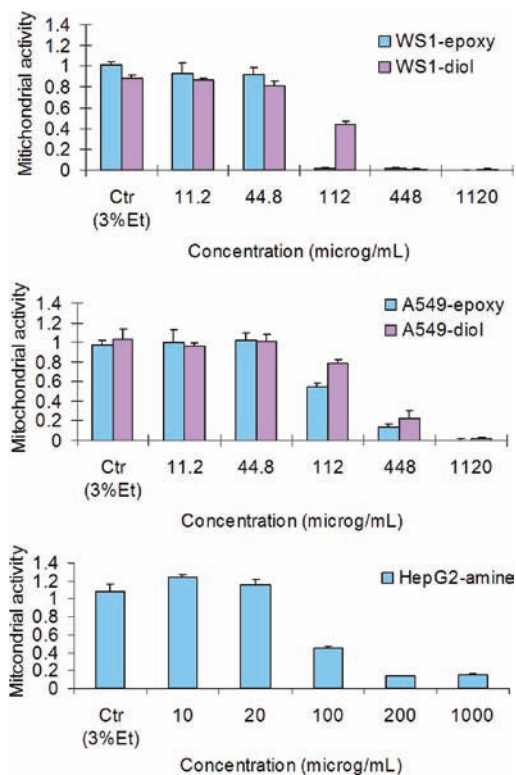


Figure 5. MTT assay of silicon quantum dots. A549 and WS1 with epoxyhexane and hexandiols capped silicon quantum dots and HepG2 with amine capped silicon quantum dots.

terminated quantum dot cytotoxicity appears at a concentration of 112 $\mu\text{g}/\text{mL}$. In comparison, the diol-terminated silicon

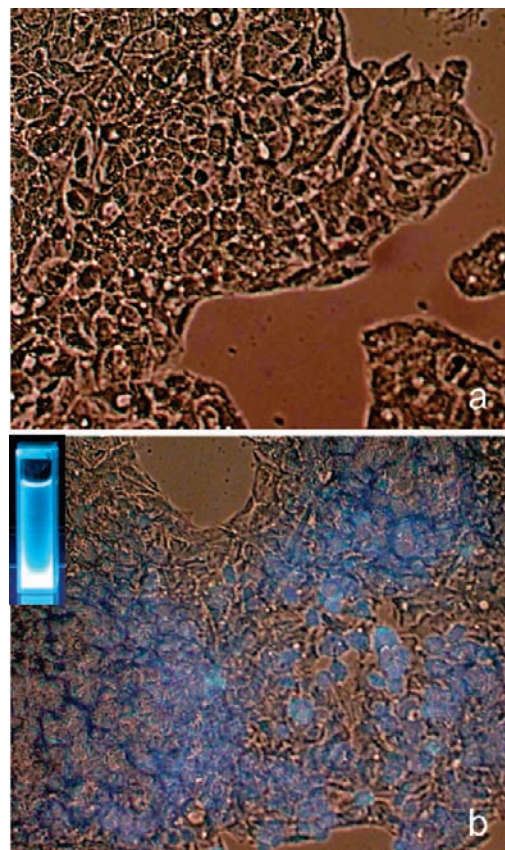


Figure 6. Cell imaging using silicon quantum dots capped with allylamine. (a) Transmitted light image and fluorescent image of negative control; (b) transmitted light image and fluorescent image of silicon quantum dots at 1.0 $\mu\text{g}/\text{mL}$, respectively.

quantum dots did not show toxicity at this level but at 448 $\mu\text{g}/\text{mL}$. The epoxide group is a highly reactive species and known to have oxidative toxicity, and so it is in agreement with expectations that it has a higher toxicity than the diol.⁵¹ The 50% inhibition coefficients of epoxide-terminated silicon quantum dots for WS1 cell and A549 cell were 0.068 and 0.13 mg/mL , respectively. In comparison, cytotoxicity for the diol-terminated silicon quantum dots did not appear up to 0.097 and 0.225 mg/mL for WS1 cell and A549 cell lines, which is almost double the concentration as compared to epoxide-terminated quantum dots. These figures are comparable to previous studies on quantum dots that have relatively low toxicity.^{52–54} The reason why the 50% inhibition coefficients of both sets of silicon quantum dots were higher for A549 than WS1 cell lines is most likely due to the difference of the metabolism of each cell line, which would affect the uptake of the silicon quantum dots.

To compare the toxicity beyond these two cell lines, toxicity on liver cell was evaluated with amine-terminated silicon quantum dots. The liver has the function to reduce toxicity by albumin secretion or glucuronate conjugation among the tissues in which quantum dots may accumulate. The results showed

(51) Hemminki, A.; Väyrynen, T.; Hemminki, K. *Chem.-Biol. Interact.* **1994**, *93*, 51–58.

(52) Chang, E.; Thekkekk, N.; Yu, W. W.; Colvin, V. L.; Drezek, R. *Small* **2006**, *2*, 1412–1417.

(53) Manzoor, K.; Johny, S.; Thomas, D.; Setua, S.; Menon, D.; Nair, S. *Nanotechnology* **2009**, *20*, 065102.

(54) Fujioka, K.; Hiruoka, M.; Sato, K.; Manabe, N.; Miyasaka, R.; Hanada, S.; Hoshino, A.; Tilley, R. D.; Manome, Y.; Hirakuri, K.; Yamamoto, K. *Nanotechnology* **2008**, *19*, 415102.

that the 50% inhibition coefficient of amine-terminated silicon quantum dots in the hepatoma cell line (HepG2) was 0.1 mg/mL, which is similar to the diol-terminated silicon quantum dots in WS1 cells. The results imply safe uses of silicon quantum dots in biological application below these concentration thresholds.

Cell Imaging. Figure 6 shows the cell imaging of silicon quantum dots capped with allylamine. This image shows the suitability of allylamine-capped silicon quantum dots as a chromophore for biological imaging. For the images in Figure 6, an excitation wavelength of 365 nm was used, and the emission at 480 nm was monitored. The control image (Figure 6a) shows minimal fluorescence from the HeLa cells relative to the HeLa cells with the incorporated silicon quantum dots (Figure 6b). Thus, the fluorescence observed in the HeLa cells in Figure 6b arises from the emission from silicon quantum dots. The inset in the top left corner of Figure 6b shows the bright blue fluorescence from a vial of allylamine capped silicon quantum dots in water when excited with UV light. The bright blue fluorescence from the silicon quantum dots is distributed uniformly and shows that the silicon quantum dots were taken up into the cytoplasm. This result shows the possibility of using

these hydrophilic silicon quantum dots as chromophores in biological fluorescence imaging.

Conclusions

Chemical reactions on the molecules attached to the surface of silicon quantum dots have been performed to produce quantum dots with reactive surface functionalities such as diols and epoxides. These quantum dots are relatively monodisperse and exhibit luminescence under UV excitation. The results from cytotoxicity studies indicate that toxicity is dependent on the surface functionality and that the silicon quantum dots as prepared have potential in biological applications such as bioimaging. This research opens the door for future biological applications of silicon quantum dots.

Acknowledgment. R.D.T. thanks the MacDiarmid Institute for funding. A.S., S.P., T.H.L., and R.D.T. thank FRST for funding through Grant IIOF VICX0601.

Supporting Information Available: TEM images and optical properties. This material is available free of charge via the Internet at <http://pubs.acs.org>.

JA906501V